Applied Thermal Engineering 131 (2018) 933–946

Contents lists available at ScienceDirect

Applied Thermal Engineering

journal homepage: www.elsevier.com/locate/apthermeng

Research Paper

Criteria for the matching of inlet and outlet distortions in centrifugal compressors

Meijie Zhang, Xinqian Zheng *

Turbomachinery Laboratory, State Key Laboratory of Automotive Safety and Energy, Tsinghua University, Beijing, China

HIGHLIGHTS

- Matching of inlet and outlet distortions has a great effect on the performance.
- The matching mechanism is analyzed.
- The criteria for the matching is proposed.
- An estimate formula for the best matching is proposed.

ARTICLE INFO

Article history:
Received 20 April 2017
Revised 26 November 2017
Accepted 27 November 2017
Available online 2 December 2017

Keywords:
Matching criteria
Inlet distortion
Outlet distortion
Centrifugal compressor

ABSTRACT

The centrifugal compressor is a very common type of effective energy conversion device, which is used in a range of industrial processing equipment and automotive turbochargers. Due to the requirements and the limited installation space, centrifugal compressors are always connected with complex inlet and outlet pipe systems, including various kinds of bends, struts, and volutes with asymmetric geometries. These asymmetric components induce distortions at the compressor inlet and the outlet, which exert a strong influence on the compressor performance and flow field. This paper employs full-annulus unsteady simulations to study the matching of inlet and outlet distortions by adding a distortion model to compressor inlet and outlet. The results show that the matching does have a large influence on the compressor performance and flow field and there does exists the best matching. The best matching can neutralize the inlet and outlet distortions, keep the uniformity of flow parameters in the impeller and the diffuser, and inhibit the oscillation of mass flow in one blade passage. In addition, the peak efficiency under the best matching can be improved 0.67% and 1.16% at 80% and 100% nominal rotation speed, respectively. Finally, the matching criteria are proposed and validated, and an estimate formula is established to provide some guidance for the installation and integrated design of compression system.

1. Introduction

Due to the common nature and effectiveness as an energy conversion device, improving centrifugal compressors' performance has great significance on the saving of energy on a large scale [1]. Distortions are important issues that should never be neglected by designers because they have a great influence on the compressor performance and stability. Distortions commonly exist in real compressor operation conditions, but the distortions concerned by people are different according to different compressor application environments.

Inlet distortion is the main issue for axial compressors due to their application on both civil and military aero-engines. Axial fans which are equipped for air-cooled heat exchangers commonly suffer from inlet flow distortion caused by inlet cross flow, and this distortion will impose adverse effect on fan static pressure rise [2]. Fidalgo et al. [3] studied fan-distortion interaction within the Rotor 67 transonic stage by experimentation and three-dimensional unsteady simulation, and discovered that the inlet distortion could lead to compressor work input variation that determines the distribution of distortion parameters downstream. Brossman et al. [4] focused on the impact of small changes in the inlet boundary conditions on a three stage compressor performance predictions and the results suggested that the tip region of first stage was most sensitive to minor changes in the inlet boundary conditions. Reuβ et al. [5] conducted an experimental investigation of coupled static and dynamic total pressure inlet distortions on a five stage high pressure compressor, and their results

* Corresponding author.
E-mail address: zhengxq@tsinghua.edu.cn (X. Zheng).

https://doi.org/10.1016/j.applthermaleng.2017.11.140
1359-4311/

Nomenclature

A	area (m^2)
Cp	constant-pressure specific heat (J/kg/K)
L	characteristic length of impeller passage (m)
N	nominal rotation speed (rpm)
O	outlet
P	pressure (Pa)
PC	pressure change (Pa)
Pr	pressure ratio (–)
R	radius (m)/gas constant (J/mol/K)
R/S	rotor/stator
T	one revolution time (s)
U	tangential velocity (m/s)
V	absolute velocity (m/s)
W	relative velocity (m/s)
Z	blade number (–)
a	sound speed (m/s)
k	specific heat ratio (–)
m	mass flow (kg/s)
n	impeller rotation speed (rpm)
t	time (s)
u	impeller tip velocity (m/s)

Greek letters

α	absolute flow angle (°)
β	blade backsweep angle (°)
δ	circumferential angle (°)
η	adiabatic efficiency (–)
θ	circumferential angle (°)
ξ	Blade stagger angle (°)
π	total pressure ratio (–)
ρ	density (kg/m^3)
σ	slip factor (–)
ϕ	inlet flow coefficient (–)
ω	total pressure loss coefficient (–)

Superscripts

–	low pressure area/average
*	stagnation
.	flow rate

Subscripts

1	impeller inlet
1t	impeller inlet blade tip
1r	impeller inlet blade root
2	impeller outlet
av	average
clean	clean flow
corr	corrected
*k*2	infinity blades outlet
low	low pressure area
m	meridional direction
t	total
ts	total to static
tt	total to total

showed the influence of distortions on the compressor operation and their interaction.

Contrary to axial compressors, centrifugal compressors are usually applied in industrial processing equipment and automotive turbochargers [6]. In real applications, the compressors are always connected with complex pipe systems or struts due to real-world requirements and limited installation space; therefore, distortions always exist at the inlet of the compressors. With the trend of high pressure ratio, the effects of distortions coupled with internal heat leakage [7] would become more serious. Bayomi et al. [8] used inlet straighteners to eliminate inlet distortions for improving centrifugal fan performance. Enayet et al. [9] took Laser-Doppler measurements of laminar and turbulent flow in a pipe bend and showed the development of a pair of counter-rotating vortices in the streamwise direction. Sudo et al. [10] took the technique of rotating a probe with an inclined hot wire and studied the turbulent flow characteristics in a circular-sectioned 90-degree bend. Lou et al. [11] used laser Doppler velocimetry to study the flow field inside a rectangular-sectioned 90° bend and showed how a small change in upstream geometry had an influence on the flow patterns of the bend. When the centrifugal compressor is connected to the pulse detonation combustor in the pulse detonation turbine engine, there will exist a pressure distortion at the compressor outlet. The study of Lu et al. [12] revealed that the distortion would change compressor operating points and push it to the surge line.

A gas collector is always necessary following a centrifugal compressor, and the gas collector is designed asymmetrically for the purpose of collecting and guiding gas. However, this asymmetrical geometry also induces distortion at the outlet of an impeller which can effect compressor performance and stability [13]. The study of Zheng et al. [14] revealed that the variation of compressor efficiency due to volute's asymmetry could be up to 4% and the outlet pressure distortion caused by the volute triggered some certain passage to stall first. Reunanen et al. [15] studied different volute geometries using a numerical method and found that the volute tongue was a more important factor for performance, meanwhile, it was also the source of outlet distortion for the compressor. To weaken the distortion caused by volute, Hariharan and Govardhan [16] designed parallel wall volutes for a centrifugal blower and their results showed that the static pressure distribution at volute inlet was more uniform and the overall performance improved 6%. Yang et al. [17] used numerical method to investigate the effect of self-recirculation-casing treatment on high pressure ratio centrifugal compressor and found that it can depress the circumferential flow distortion in the impeller. Zheng et al. [18], using an experimental and numerical method, studied the asymmetric flow in a high pressure ratio turbocharger centrifugal compressor induced by the volute and develop a corresponding asymmetric self-recirculation casing treatment as a flow control method to minimize the asymmetric flow.

Concluding from the above research, we can see three main relevant findings:(1) Inlet distortion has a great influence on both axial and centrifugal compressors; (2) Because of upstream inlet bends, struts, guide vanes and downstream asymmetric volute geometry, there exits inlet and outlet distortions in centrifugal compressors; (3) Lowering the flow parameters' non-uniformities can achieve better performance and stability. A special situation should be noted that there are inlet and the outlet distortions in centrifugal compressors, but the influence of the relationship and interaction of the inlet and outlet distortion on the performance and stability is not well covered in previous research.

This study was mainly focused on the matching of inlet and outlet distortion. In this paper, two different square wave distortions are added to the inlet and outlet of a compressor, respectively. The circumferential position of the outlet distortion is fixed, and the inlet distortion's circumferential position was changed to study the influence of the matching between the inlet and outlet

distortion on compressor performance and flow field. In order to capture the distortion's transfer characteristics, all calculations of this study adopt full-annular unsteady simulations. Finally, the criteria of the best matching for compressor performance are proposed based on the matching mechanism and validated, an estimate formula for inlet distortion angular shift thus providing some guidance on the integrated compression system design including inlet pipe systems, compressors and volutes.

2. Computational model and approach

2.1. Compressor model

The compressor studied in this paper comes from an open test case *RADIVER*, whose experiments were conducted in the Institute of Jet Propulsion and Turbomachinery at RWTH Aachen, Germany. *RADIVER* is a single stage centrifugal compressor with a wedge diffuser, but there are some experimental data of *RADIVER* with a vaneless diffuser at 0.8 nominal rotational speed. Based on the experimental data for numerical validation, the *RADIVER* compressor with a vaneless diffuser at 0.8 nominal rotational speed is employed for the study of this paper. The main characteristic parameters of this compressor are given in Table 1.

The full-annulus computational domain can be divided into three zones by two Rotor/Stator (R/S) interfaces: the upstream inlet, the centrifugal impeller, and the diffuser, as shown in Fig. 1. Due to the asymmetric nature of the inlet and outlet distortion, it is necessary for the computational domain to contain the whole compressor stage. To reach the required mesh standard of unsteady computation and achieve a high mesh quality, the O4H topology structure is employed to create compressor grids. One blade passage is divided into five blocks: the inlet block, the outlet block, the up block, the down block and the skin block. Except for the skin block, which adopts an O-type mesh structure, the other 4 blocks all adopt an H-type mesh structure, seen in Fig. 1.

The final total grid size was approximately 7.2 million and the resulting Y^+ of solid walls, including blade surfaces, hub and casing walls, all values within 5 in most flow regions.

Table 1
Compressor characteristic parameters.

Parameters	Values
Nominal rotation speed N	35,200 rpm
Number of blades Z	15
Blade backsweep angle β_{k2}	38 °
Impeller inlet tip radius R_{1t}	72.9 mm
Impeller inlet root radius R_{1r}	30.3 mm
Impeller outlet tip radius R_2	135 mm
Shroud radius at impeller inlet	72.9 mm
Hub radius at impeller inlet	30.1 mm
Tip radius at impeller outlet	135 mm
Tip clearance at impeller leading edge	0.7 mm
Tip clearance at impeller trailing edge	0.48 mm
Straight vaneless diffuser width	11.2 mm

2.2. Distortion model

Contrary to the uniform flow hypothesis of design procedure, compressors in reality always operate at various distortion flow conditions. Due to axial compressors' common application to aero-engines, most investigations of inlet flow distortion are concentrated on axial compressors. Many experiments have been designed and many models have been developed to research the influence of inlet distortion on the instability and performance of axial compressors. Compared with the frequent research on axial compressors, the concern for centrifugal compressor is much lower. The advantages of high pressure ratio and rotation speed result in centrifugal compressors being much more commonly used in automotive engines. The complex piping system caused by limited installation space, the broader operation conditions and asymmetrical gas collecting devices lead to more severe flow distortions at the inlet and outlet of centrifugal compressors.

Considering the distortion pattern, range and intensity in automotive engine operation, the inlet and outlet distortion pattern were ultimately determined to be circumferential 60° square waves, where the inlet distortion is of total pressure and the outlet distortion is of static pressure. The distortion intensity index is 8.5% for inlet distortion and 4.2% for outlet distortion [19,20]. The distortion intensity index is defined by [21]

$$\frac{\Delta PC}{P} = \frac{P_{av} - P_{av,low}}{P_{av}} \tag{1}$$

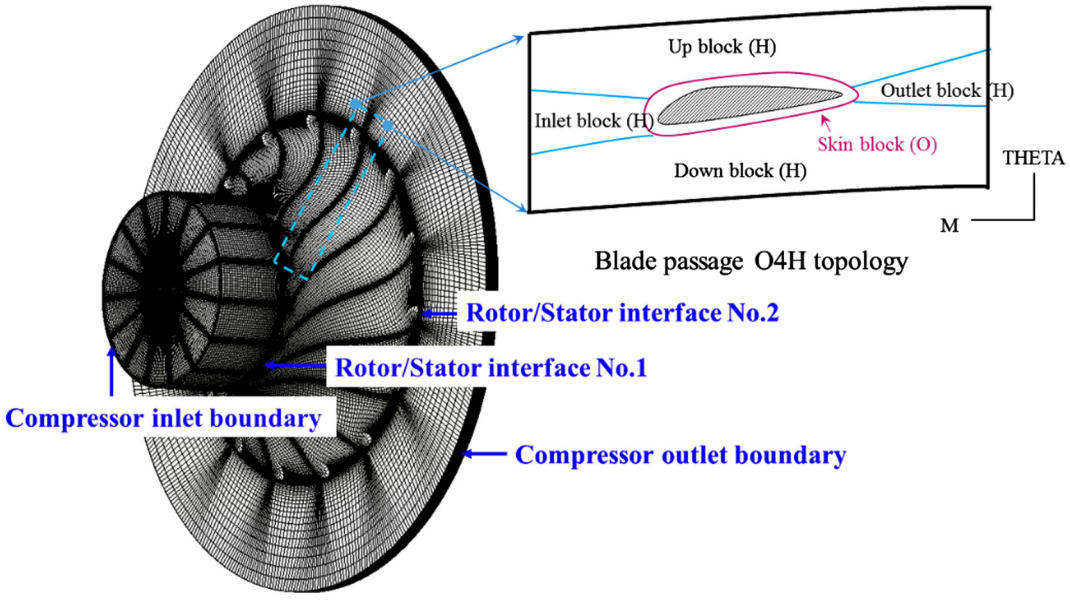

Fig. 1. Full-annulus computational mesh.

where P_{av} is the averaged pressure for one ring surface and $P_{av,low}$ is only for the low pressure area.

$$P_{av} = \frac{1}{360}\int_0^{360} P(\theta)d\theta \tag{2}$$

$$P_{av,low} = \frac{1}{\theta^-}\int_{\theta^-} P(\theta)d\theta \tag{3}$$

where θ^- is the circumferential degree of low pressure area.

In the matching study of inlet and outlet distortions, the circumferential position of the outlet distortion is fixed, but the circumferential position of the inlet distortion changes 60° sequentially for each case. Fig. 2 shows the distributions of the inlet total pressure and the outlet static pressure as well as the pattern and amplitude of distortions [3,22]. For clarity and simplification, the circumferential angle between inlet and outlet distortion δ is defined from the middle of outlet distortion to the middle of inlet distortion, $0° < \delta < 360°$. For example, δ = 120° in the case shown in Fig. 2.

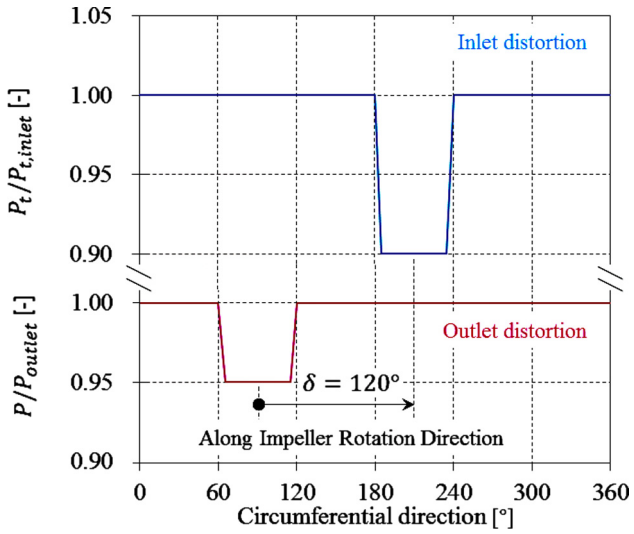

Fig. 2. Distortion distribution of inlet total pressure and outlet static pressure.

2.3. Numerical method and validation

All simulations of this study are time-consuming but more accuracy unsteady full-annular calculations in order to capture the interaction characteristics between inlet and outlet distortions. The CFD solver employed in this study is EURANUS integrated in FINE software package of NUMECA, which is used to solve the unsteady, compressible, Reynolds-averaged, Navier-Stokes equations on structured grids by a finite volume approach. The spatial discretization is based on a central scheme and the time marching is four-order Runge-Kutta scheme. The flow governing equations are enclosed with Spalart-Allmaras, a one-equation turbulence model. In addition to these methods, an explicit dual time-stepping procedure is employed in the unsteady computation to achieve an efficient and time-accurate solution and the inner iteration step is set to 30. The unsteady computations with sliding mesh at Rotor/Stator(R/S) interface No. 1 and No. 2 started from initial solutions obtained from corresponding steady calculations. The number of physical time steps per period was 180, so one physical time step is corresponding to $1.18e^{-5}$ s. Totally 2700 physical time steps, 15 rotation periods, are performed to obtain a converged solution. Absolute total pressure, absolute total temperature and velocity direction are imposed as the inlet condition and the turbulent viscosity is $1e^{-4}$ m^2/s. The outlet condition is a given static pressure and The wall condition is non-slip and adiabatic. The performance line of constant rotation speed is obtained by gradually increasing the compressor outlet static pressure, but the distortion intensity index is always a constant.

The comparison of impeller total pressure and impeller efficiency between unsteady simulation results and experiment data [23] is shown in Fig. 3. This is conducted in clean flow (without inlet and outlet distortions), at 0.8 *N* rotation speed. The abscissa ϕ_{corr} is a corrected global inlet flow coefficient defined by

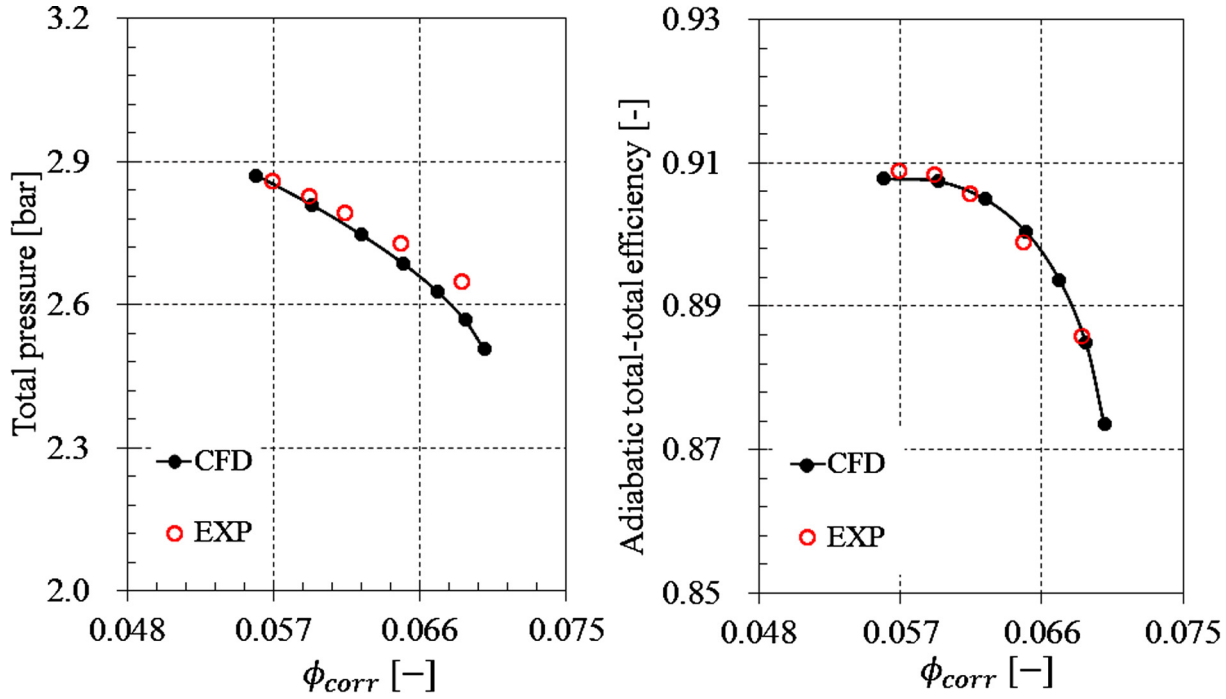

Fig. 3. Impeller total pressure and efficiency comparison between unsteady simulation results and experiment data in clean flow.

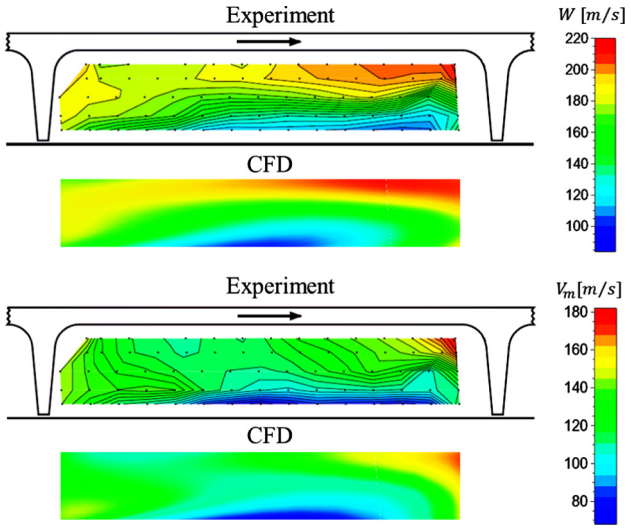

Fig. 4. Time-averaged relative velocity and meridional velocity of impeller outlet comparison in clean flow.

$$\phi_{corr} = \frac{\dot{m}_{corr}}{\rho_{t1} D_2^2 u_2} \tag{4}$$

$$\dot{m}_{corr} = \dot{m} \sqrt{\frac{T_t}{T_{t,ref}}} \frac{P_{t,ref}}{P_t} \tag{5}$$

where $\dot{m}_{corr}$ is corrected mass flow, ρ_{t1} is inlet total density, D_2 is blade outlet tip diameter and u_2 is blade outlet tip speed, T_t is compressor inlet total temperature and P_t is compressor inlet total pressure. In this paper, $T_{t,ref}$ is 288.15 K, P_t is 101300 Pa.

Fig. 4 shows the detailed time-averaged flow field, relative velocity W and meridional velocity V_m, of impeller outlet at $\phi_{corr} = 0.057$. Compared to experimental data which is obtained by Laser-2-Focus measurements, numerical results have captured all of the main flow characteristics, including the low relative velocity and meridional velocity near the shroud which are effected by tip clearance flow. The impeller performance and flow field comparisons, in Figs. 3 and 4, demonstrate that the compressor model and the numerical method are credible.

3. Performance under different matching

The main purpose of this section is to investigate how the performance varies with the different matching of inlet and outlet distortions. So unsteady numerical simulations are employed for six cases and the results of compressor isotropic efficiency and total-static pressure ratio under different matching are shown in Fig. 5. It demonstrates that different matching of inlet and outlet distortions does have evident performance differences. The efficiency difference between case δ = 0 ° and case δ = 60 ° at highest efficiency points (optimum Pr_{ts} points) is 0.67%, and when the mass flow decreases, the difference increases up to 1.69% at 1.04 optimum Pr_{ts} point.

The compressor studied in this paper is composed of an impeller and a vaneless diffuser. Analyzing component performance is always a very useful tool to help one learn what occurred in a system. Fig. 6 gives the impeller total-total isotropic efficiency and diffuser total pressure loss coefficient change relative to clean flow condition. With the decrease of mass flow, the influence of distortion is becoming stronger, so the impeller efficiency change of six cases relative to clean flow condition are all increasing. At the same time, the effect of distortion matching is also becoming greater with the decrease of mass flow, as shown in Fig. 6(a). With the decrease of mass flow, the diffuser total pressure loss coefficient has the same variation trend, except for case δ = 0° whose diffuser total pressure loss coefficient keeps almost the same as the clean flow condition, as shown in Fig. 6(b). It proves that the matching of case δ = 0 ° can suppress the negative effect of distortions on the impeller and diffuser performance and there does exist a best matching of inlet and outlet distortions for compressor performance.

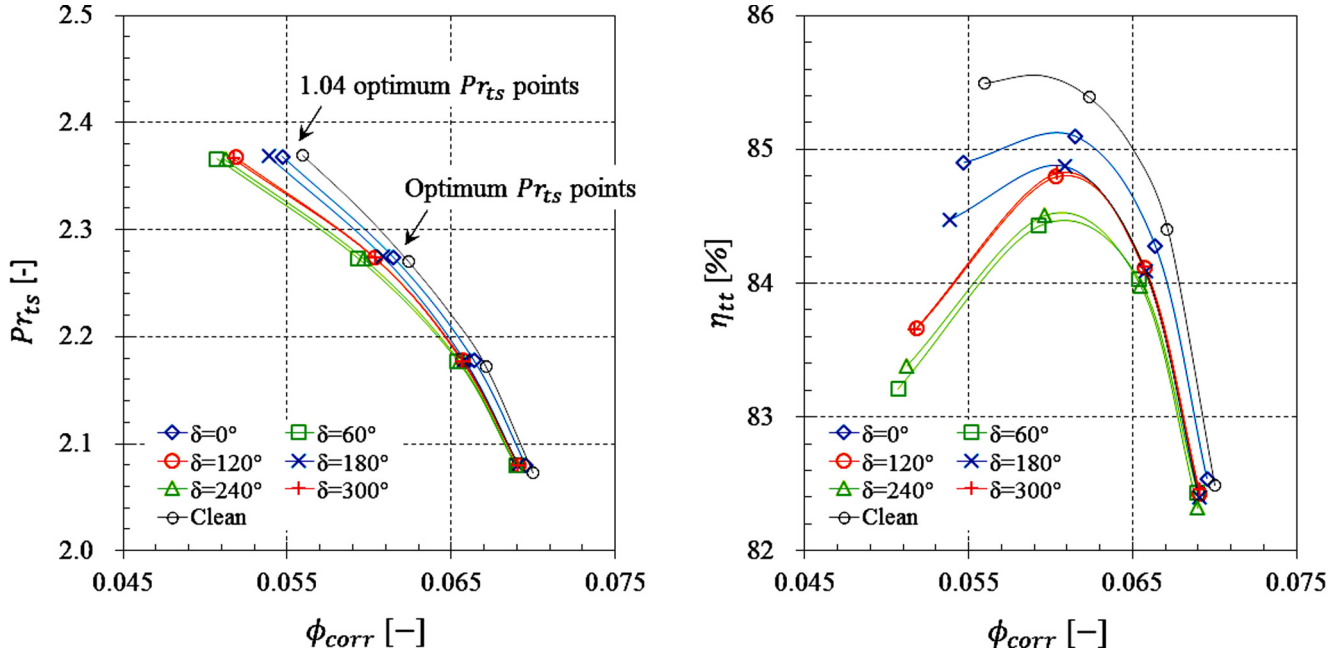

Fig. 5. Compressor isotropic efficiency and total-static pressure ratio comparison under different matching.

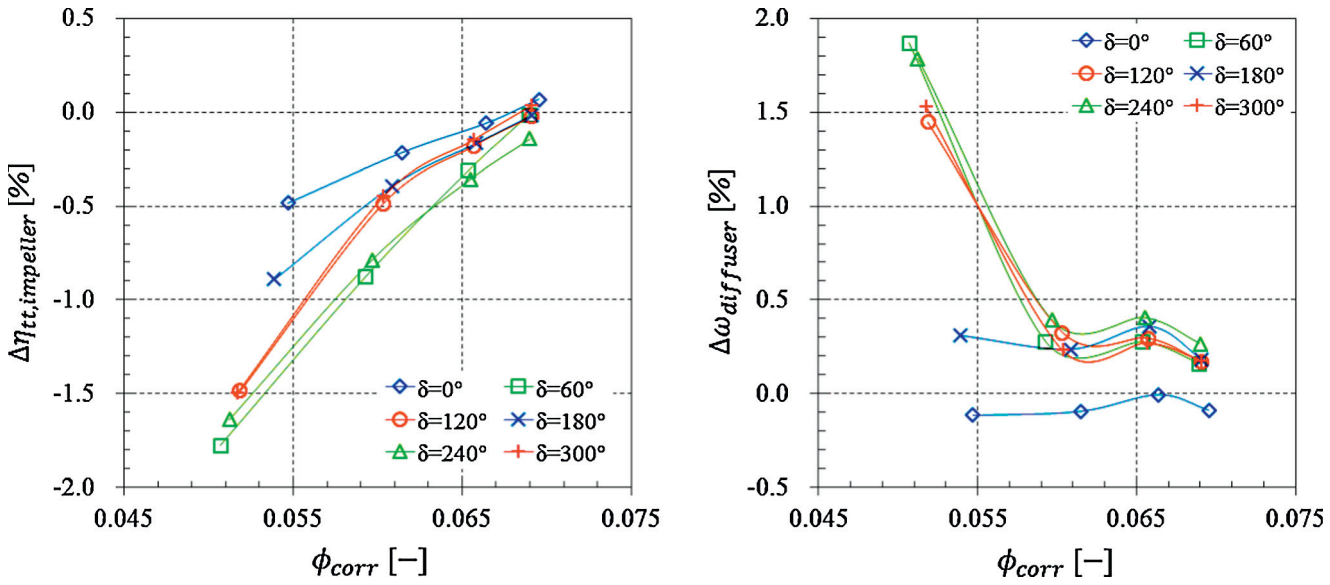

(a) Impeller total-total isotropic efficiency

(b) Diffuser total pressure loss coefficient

Fig. 6. Components performance under different matching of inlet and outlet distortions by unsteady simulations.

4. Matching mechanism and criteria

4.1. Matching effect on impeller

The boundary condition is foremost among those factors which are related to compressor operation condition, and a good boundary condition is crucially important for the impeller and diffuser performance. For a compressor, there are three important conditions. The first is the impeller inlet boundary condition, the second is the impeller outlet (diffuser inlet) boundary condition, and the last is the diffuser outlet boundary condition. For distortion studies, because the impeller inlet and the diffuser outlet boundary conditions are always controlled by upstream and downstream components, the parameter distribution at impeller outlet (diffuser inlet) becomes more important. It is the distortion angular shift that leads to the performance difference under different matching of inlet and outlet distortions. To clearly capture the angular shift characteristics of inlet distortion and outlet distortion, Fig. 7 gives the angular shift between impeller inlet and outlet. The distorted pressure wave is similar to the sound wave [20], and its propagation speed is related to the local sound speed and the local fluid flow speed. So the propagation speed of inlet distorted pressure wave, from impeller inlet to outlet, is larger than that of outlet distorted pressure wave, from impeller outlet to inlet. Fig. 7(a) shows the angular shift of minimum static pressure from impeller inlet to outlet at 1.04 optimum Pr_{ts} is around 65° when only inlet total pressure distortion exists, and what should not be overlooked is that a wave peak of static pressure, near 180°, appears at the

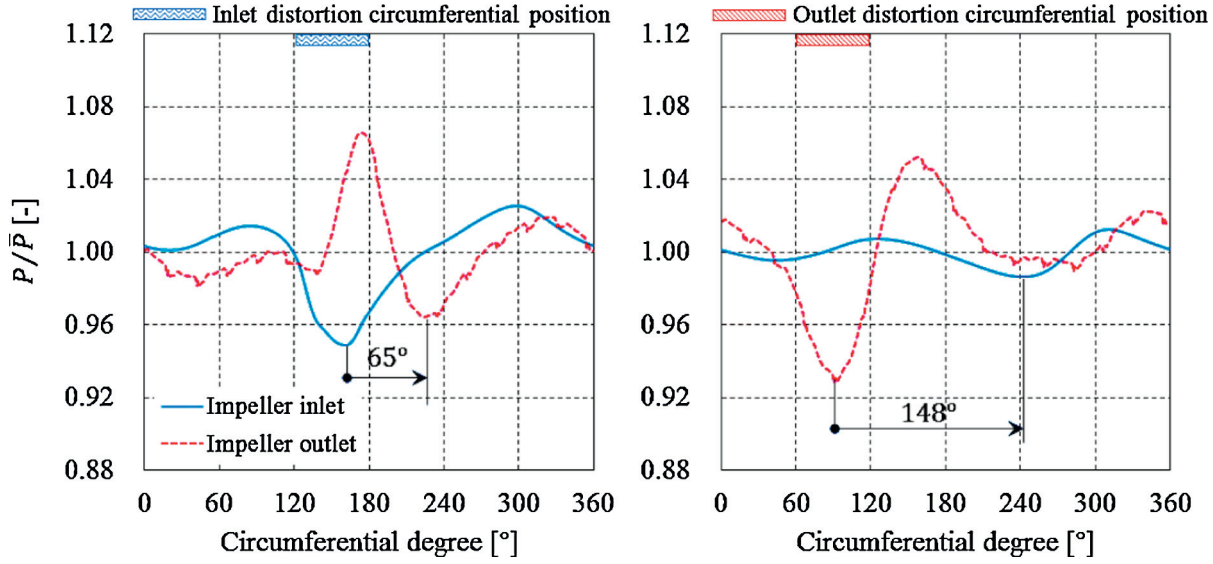

(a) only existing inlet distortion

(b) only existing outlet distortion

Fig. 7. Time-averaged static pressure distributions of 50% span along circumferential direction at the impeller inlet and the impeller outlet for single distortion at 1.04 optimum Pr_{ts} point (the impeller rotation direction is from 0 to 360°).

impeller outlet at the same time (It is caused by the reduce of mass flow in some blade passages and will be discussed in the later section). Fig. 7(b) shows the angular shift of minimum static pressure from impeller outlet to inlet at 1.04 optimum PR_{ts} is around 148° (Because the perturbation wave propagates against air flow, the angular shift is larger) when only outlet static pressure distortion exists, and there is also a distinct wave peak, near 150°, at the impeller outlet. Compared to the inlet pressure amplitude change caused by the outlet distortion, the outlet pressure amplitude change caused by the inlet distortion is much larger, so it is also reasonable to pay more attention on outlet static pressure distribution.

Taking angular shift into consideration, the parameter distributions at impeller outlet (diffuser inlet) appear diverse for the different matching of inlet and outlet distortions. Fig. 8 shows the time-averaged static pressure distribution of 50% span along circumferential direction at the impeller inlet and the outlet for the different distortion matching. Looking at the high performance cases, such as case $\delta = 0^\circ$, the inlet distortion transfer weakens the outlet inherent wave peak of static pressure, making the outlet static pressure more uniform. On the contrary, that worse performance cases, such as case $\delta = 60^\circ$ and case $\delta = 240^\circ$, the inlet distortion transfer strengthens the outlet inherent wave peak or trough of static pressure, making the outlet static pressure more non-uniform. For example, the two wave peaks at impeller outlet caused by the inlet distortion transfer and the outlet distortion respectively superpose each other in case $\delta = 60^\circ$, while the two wave troughs at impeller outlet caused by the inlet distortion transfer and the outlet distortion respectively produce a wider wave tough in case $\delta = 240^\circ$. This is responsible for the impeller and diffuser performance differences, as shown in Fig. 6, for the different matching of inlet and outlet distortions.

It can be clearly seen that the pressure matching at impeller outlet can be divided into three types. The first matching type is that there is an interaction between the inlet distortion transfer and the outlet distortion, and it weakens each other, so the impeller efficiency is better, such as case $\delta = 0^\circ$ and $\delta = 180^\circ$; the second matching type is that there is also an interaction between the inlet distortion transfer and the outlet distortion, but it superposes each other, so the impeller efficiency is worse, such as case $\delta = 60^\circ$ and case $\delta = 240^\circ$; the third matching type is that there is a weak interaction or no interaction between the inlet distortion transfer and the outlet distortion, and the impeller efficiency falls in between the first and the second matching type, such as case $\delta = 120^\circ$ The impeller efficiency is always closely related to total pressure and total temperature, which can be proved by the efficiency definition. Fig. 9 shows the time-averaged total pressure and total temperature distributions of 50% span along circumferential direction at the outlet for two typical cases at 1.04 optimum Pr_{ts} point. It demonstrates that the total parameters distribution tendency is the same as the static parameters distribution, that is to say, when the static pressure distribution is better or worse, the total pressure and total temperature distributions are also correspondingly better or worse, just like case $\delta = 0^\circ$ and case $\delta = 60^\circ$ shown in Fig. 9 It proves that the impeller outlet static pressure matching can be used as a criterion for impeller efficiency.

4.2. Matching effect on diffuser

It has been shown that the impeller outlet (diffuser inlet) parameters distributions are different under the different matching of inlet and outlet distortions; thus, it is inevitable that the flow in the diffuser will have distinctive characteristics. As shown in Fig. 6, the matching can also affect diffuser performance. To expound the effect of distortion matching on diffuser performance, Fig. 10 shows the time-averaged radius velocity $V_r/V_{r,clean}$, absolute flow angle α_2 and the axial component of absolute velocity curl $Curl(V)\_z$ at 50% span in the diffusers of case $\delta = 0^\circ$ and case $\delta = 60^\circ$, at 1.04 optimum Pr_{ts} point.

As discussed in Figs. 8 and 9, the circumferential distributions of static and total parameters are non-uniform and diverse. Thus, the corresponding radius velocity in the diffuser along the circumferential direction is also non-uniform, which would deteriorate the flow performance in the diffuser. Compared to case $\delta = 60^\circ$, the distribution of the radius velocity of case $\delta = 0^\circ$ is much improved and becomes more uniform, as seen in Fig. 10(a). The reason for this is that the low energy fluid (low radius velocity) coming from the outlet of the impeller encounters the low static pressure resulting from the outlet distortion, then the lower reversed pressure gradient makes the low energy flow easier to pass through the diffuser, which produces something like a suction effect.

When the mass flow decreases, the absolute flow angle at the impeller outlet will increase. This means that the fluid will take a longer route in the diffuser which causes more energy loss (due to friction) and it is also easier to induce flow instability of the whole compressor. For the mass flow non-uniform distribution at the impeller outlet, the corresponding absolute flow angle of case $\delta = 60^\circ$ is still asymmetric and the difference can be up to nearly 20°, as seen in Fig. 10(b), which is a threat to compressor efficiency and flow stability. The matching of case $\delta = 0^\circ$ homogenizes the circumferential mass flow, so the absolute angle distribution is more uniform. The outlet distortion's suction effect of case $\delta = 0^\circ$ can also be seen in Fig. 10(b), where the absolute flow angle is high at the impeller outlet but immediately decreases upon encountering the outlet distortion.

Where there is a velocity difference for fluid, there will be a vorticity. Due to the distortions, the distributions of radius velocity and tangential velocity in the diffuser are both asymmetric, which would lead to different vorticities, as shown in Fig. 10(c). The positive curl value means the vorticity rotational direction is the same as the impeller, while the negative curl value means that it is contrary to impeller. The vorticity is a form of energy dissipation and would disturb the normal flow. Nevertheless, there are a wide range of vorticities in the diffuser of case $\delta = 60^\circ$, which should be responsible for its performance deterioration.

4.3. Matching effect on transient mass flow

Because of the inlet total pressure distortion, the inlet static pressure and mass flux distribution along the circumferential direction all become asymmetric. Limited by centrifugal compressor geometry and current measurement technology, it is still very difficult to monitor the internal mass flow of turbomachinery by experiment methods, though the situation has been eased by virtue of 3-D unsteady simulation. Even so, an interesting phenomenon is observed with the help of 3-D unsteady simulation. Owing to the asymmetric distribution of the inlet mass flow and the fluid inertia, the inlet mass flow and the outlet mass flow of one blade passage are unequal and the unequal distribution varies with the revolution of the one passage.

Fig. 11 shows the transient inlet and outlet mass flow fluctuations of one blade passage in a rotation period of cases $\delta = 0^\circ$ and $\delta = 60^\circ$, where the "+" sign means blade passage mass flow increased, i.e., inlet mass flow is larger than outlet, and the "−" sign means blade passage mass flow decreased, i.e., inlet mass flow is smaller than outlet. When the blade passage inlet rotates into the inlet total pressure distortion area, the inlet mass flow will immediately drop, while the outlet mass flow cannot respond to the variation of the inlet immediately due to flow inertia. Then, the blade passage inlet leaves the inlet distortion area and inlet

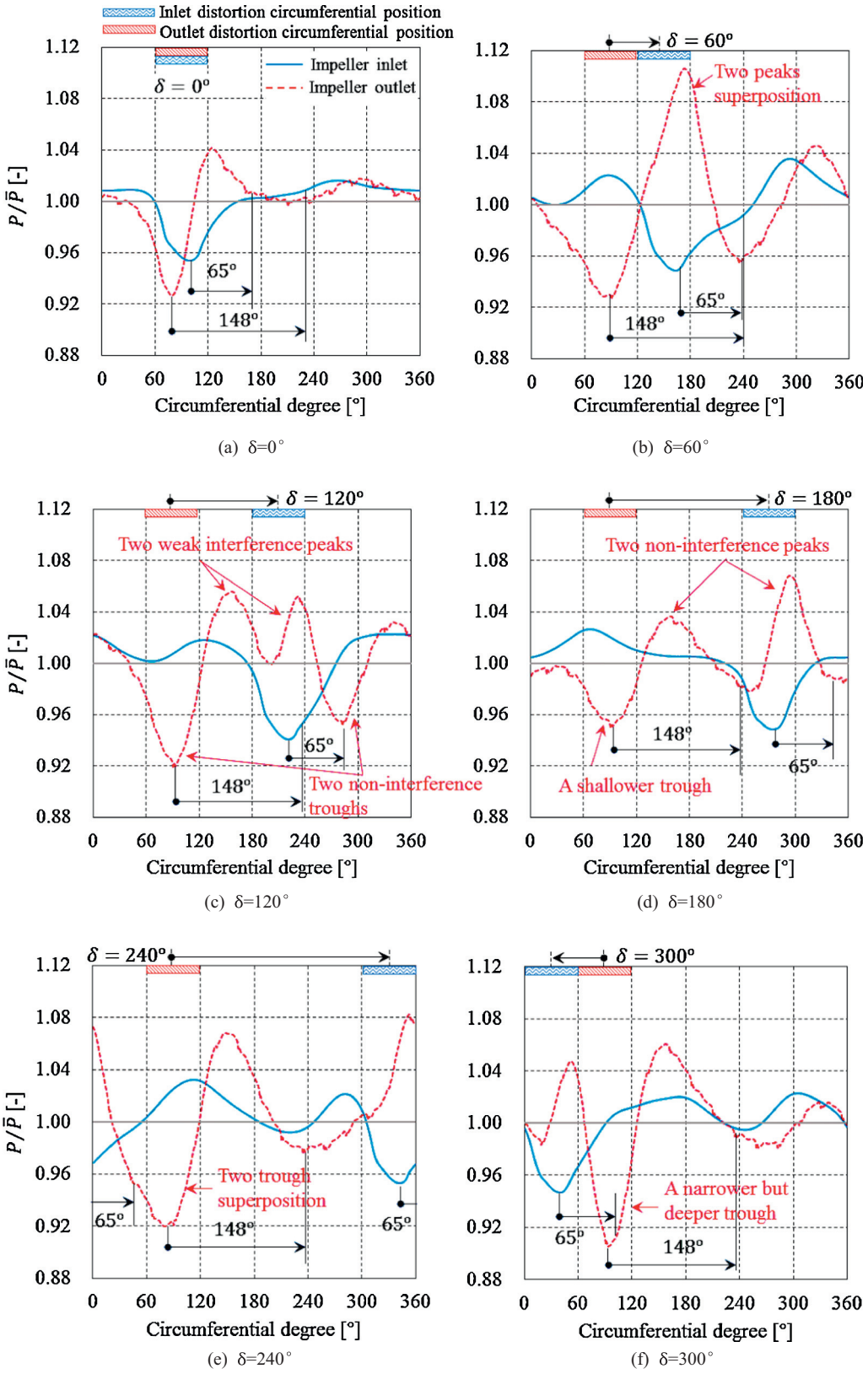

Fig. 8. Time-averaged static pressure distributions of 50% span along circumferential direction at the impeller inlet and the impeller outlet for different matching at 1.04 optimum Pr_{ts} point (the impeller rotation direction is from 0 to 360°).

mass flow also recovers from distortion. The outlet mass flow does not drop until this moment. The asynchronous variation of the inlet and outlet mass flow leads to the periodic increase and decrease of flow mass in one blade passage. This would make blade work input unsteady and cause blade work input loss. When a compressor is working at near the surge point, this phenomenon

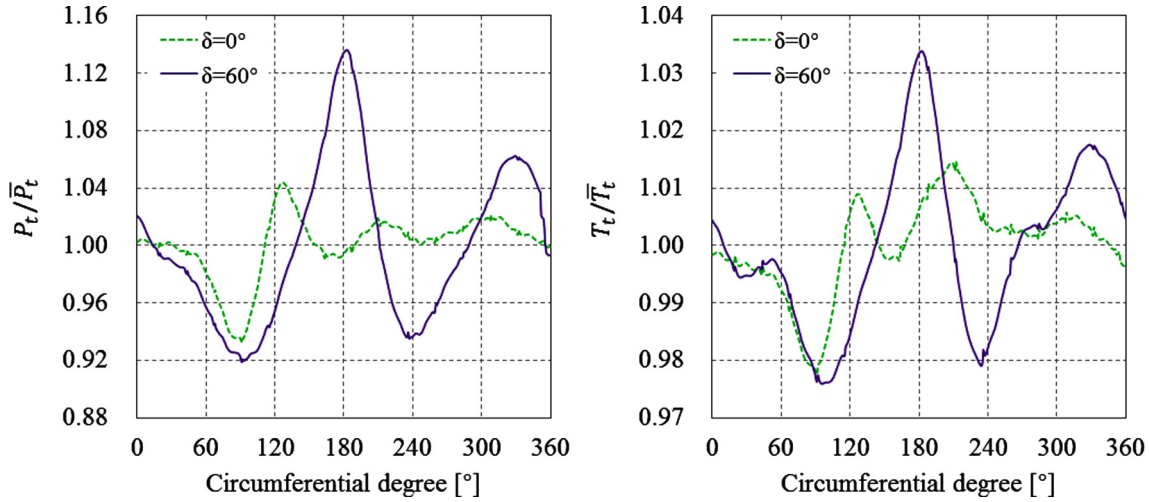

Fig. 9. Time-averaged total pressure and total temperature distributions of 50% span along circumferential direction at the impeller outlet for two typical cases at 1.04 optimum Pr_{ts} point.

would become very harmful to the compressor flow stability because it could induce backflow in several blade passages in advance. The match of case δ = 0° limits the mass flow fluctuation amplitude and range to an acceptable range. Except for the inlet distortion area, the inlet and outlet mass flow are nearly identical at other circumferential positions. Nevertheless, the mass flow fluctuation of case δ = 60° exists in the whole rotation period, and the amplitude is much larger than that of case δ = 0°.

4.4. Matching criteria and validation

Through the discussion above, it is clear that the matching of the inlet and outlet distortion has a large influence on the performance of centrifugal compressors. The flow parameters distribution of impeller outlet (diffuser inlet) boundary is very important because it is directly related to the impeller and the diffuser performance. The inlet pipe systems always cause a total pressure distortion at the compressor inlet, and the gas collectors, such as volutes, would cause a static pressure distortion at the compressor outlet which leads to a static pressure decrease at the impeller outlet. For the inlet distortion, there is no apparent angular shift before impeller inlet. Similarly, the angular shift for the outlet distortion from diffuser outlet to diffuser inlet (impeller outlet) is also not apparent. The angular shift mainly occurs in the impeller, due to the impeller rotation. Considering that the transfer characteristics and the angular shift of inlet and outlet distortions, there exists the best matching, where the distortions have an interaction to neutralize each other (peak and trough superpose) and limit the distortion region to a minimum at impeller outlet (diffuser outlet), so it is an expected matching. This can be used as the matching criteria for inlet and outlet distortions. The avoided matching is that the distortions have an interaction to superpose each other (peaks or troughs superpose) and lead to a large fluctuating parameter distribution at impeller outlet (diffuser inlet). The mediocre matching is that the distortions have no interference and the compressor performance of this matching falls in between the best matching and the avoid matching. The sketch map of different matching types is shown in Fig. 12 Of course, the relative phase between the inlet and the outlet distortions for the best matching is not fixed, and it related to the characteristic length of impeller passage in streamwise direction, the impeller rotation speed, the circumferential width of inlet and outlet distortions, but the physical mechanism for the matching criteria that limiting the distortion amplitude and region to a minimum is the same.

In order to validate the matching criteria, the compressor performance for different matching at nominal rotation speed (N) was also studied. Fig. 13 gives two typical cases (δ = 60° and δ = 345°) performance comparison. The difference of highest efficiency between case δ = 60° and case δ = 345° is 1.16%, and the instability point of case δ = 60° has been reached around ϕ_{corr} = 0.069. This can be understood that the influence of distortion matching is becoming stronger with compressor rotation speed increase.

Time-averaged static pressure distributions of 50% span along circumferential direction at the impeller inlet and the impeller outlet for different matching at nominal rotation speed are also given in Fig. 14 Two peaks superposition is still be observed in case δ = 60° and the interaction between inlet distortion transfer and outlet distortion to neutralize each other is also observed in case δ = 345°. The results demonstrate the matching criteria shown in Fig. 12 is credible.

The key to understand the matching of inlet and outlet distortions is to grasp how the distortions transfer in the impeller and the critical factor of how can we get the best matching is to know the angular shift of inlet distortion. It can be noticed that the angular shift of inlet distortion is not fix, the angular shift Δθ is 65° at 0.8 nominal rotation speed but is 85° at nominal rotation speed. To get the best matching or at least avoid the worst matching, here an estimate formula for Δθ is given. Although the formula is simple and rough, it can speedily give a right direction. The distorted pressure wave is similar to the sound wave [20], and its propagation speed is related to the local sound speed and the local fluid flow speed. So the angular shift Δθ (*degree*) can be calculated by

$$\Delta\theta = \frac{L}{V_{wave,avg}} \times \frac{n}{60} \times 360 \tag{6}$$

where n is the impeller rotational speed, L is the characteristic length of impeller passage, $V_{wave,avg}$ is related to local sound speed and local fluid flow speed.

The highest efficiency point is always most concerned, so the parameters for estimate Δθ all come from clean flow compressor highest efficiency point. When the pressure wave passing through the blade passage, the sound reflection will occur. In addition, because the blade passage is curved and expansive, the sound incidence angle i from impeller inlet to outlet is increasing. On the contrary, the sound incidence angle i from impeller outlet to inlet is

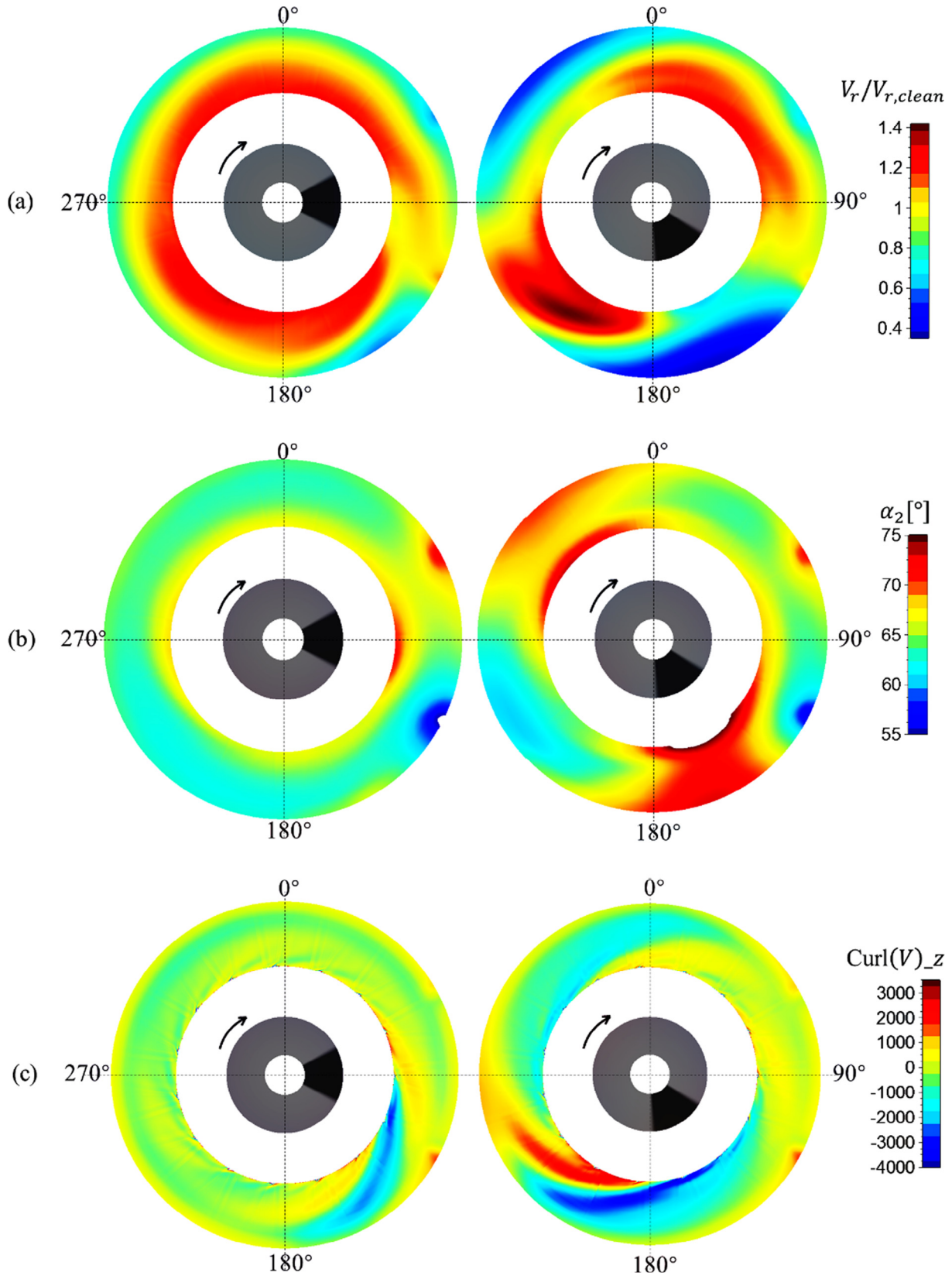

Fig. 10. Time-averaged radius velocity (a), absolute flow angle (b) and axial component of absolute velocity curl (c) at 50% span in the diffusers of case δ = 0° (left) and case δ = 60° (right) at 1.04 optimum Pr_{ts} point.

decreasing, so some outlet distortion pressure waves are reflected totally and cannot reach the impeller inlet, like shown in sketch map Fig. 15 (the real pressure wave propagation is not straight, which depends on the local density and temperature. Here is only a sketch and assume that the pressure wave is a plane wave, but it is proper to understand the process). It's one of the reasons why

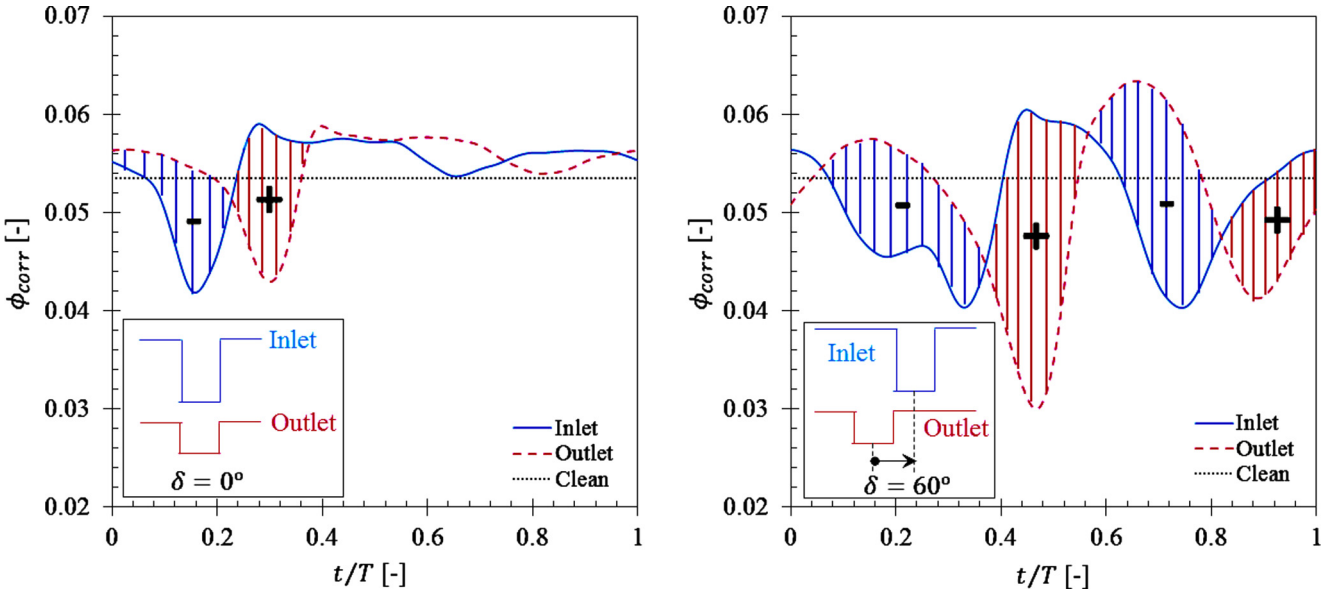

Fig. 11. Transient inlet and outlet mass flow fluctuations of one blade passage in a rotation period at 1.04 optimum Pr_{ts} point.

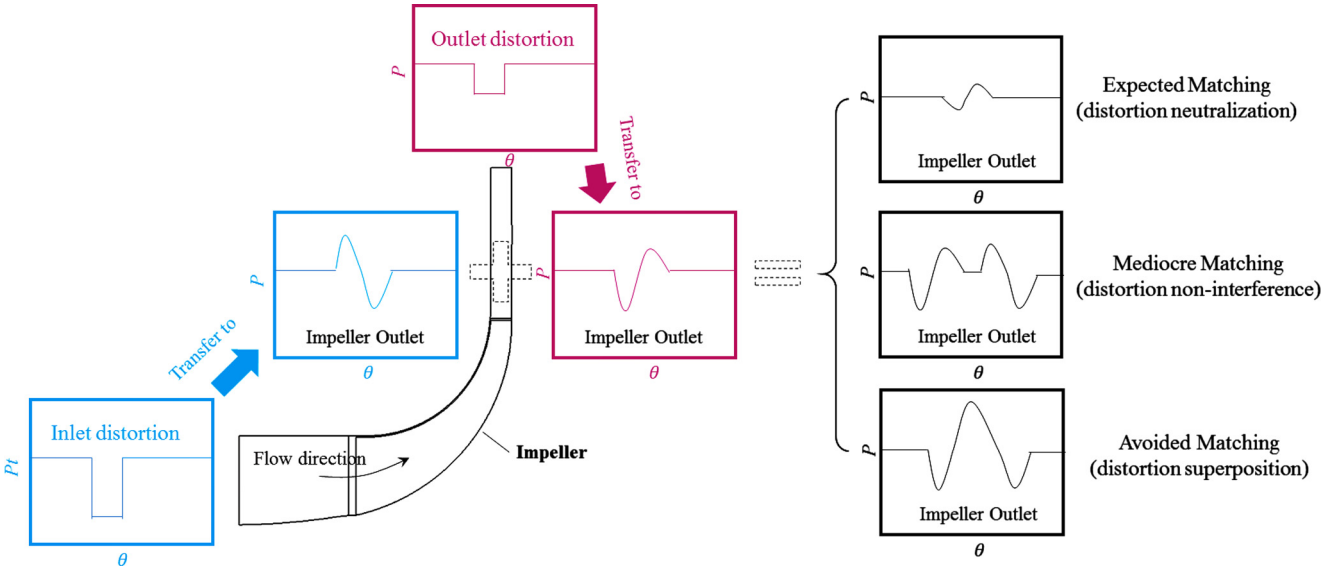

Fig. 12. Sketch map of different matching types.

the amplitude of outlet distortion become much smaller when it reaches impeller inlet, while the amplitude of inlet distortion almost the same when it reaches impeller outlet, shown in Fig.7. Considering the sound reflection and blade passage geometry characteristics, the averaged wave speed is defined by

$$V_{wave,avg} = \left(\left(\frac{a_1 + a_2}{2}\right) + \left(\frac{W_1 + W_2}{2}\right)\right) \times \cos(\xi) \tag{7}$$

$$a_1 = \sqrt{kRT_1} \tag{8}$$

$$a_2 = \sqrt{kRT_2} \tag{9}$$

where a_1 and a_2 are impeller inlet and outlet sound speed, respectively. W_1 and W_2 are impeller inlet and outlet relative flow speed, respectively. ξ is blade stagger angle and $\cos(\xi)$ is used as a correction to embody the effect of sound reflection.To estimate impeller outlet static temperature T_2, the impeller work input (T_2^*) is needed.

$$T_2^* = T_1^*(\pi^{(k-1)/k} - 1)/\eta + T_1^* \tag{10}$$

$$T_2 = T_2^* - \frac{V_2^2}{2Cp} \tag{11}$$

When to estimate impeller outlet absolute flow speed V_2, the slip factor σ [24] is considered.

$$V_{m1} = \dot{m}/(\rho_1 A_1) \tag{12}$$

$$U_1 = n/60 \times 2\pi \times R_{1,avg} \tag{13}$$

$$W_1 = \sqrt{V_{m1}^2 + U_1^2} \tag{14}$$

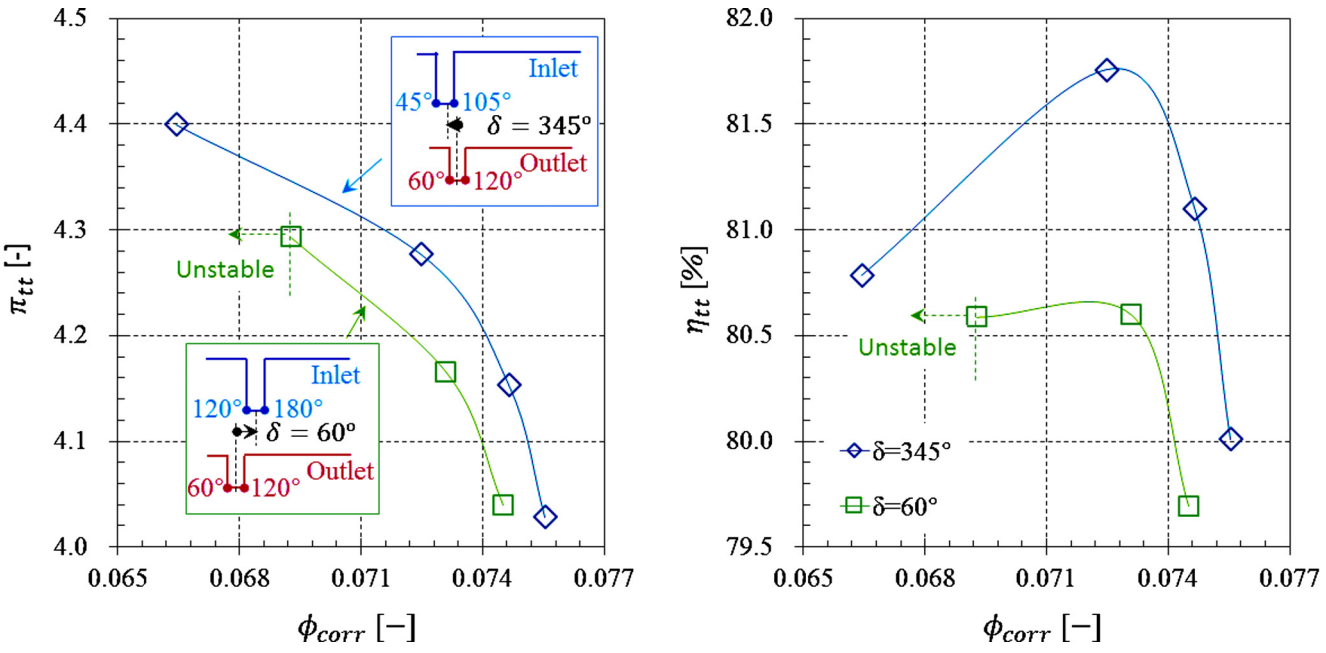

Fig. 13. Compressor performance comparison of case δ = 60° and case δ = 345° at nominal rotation speed.

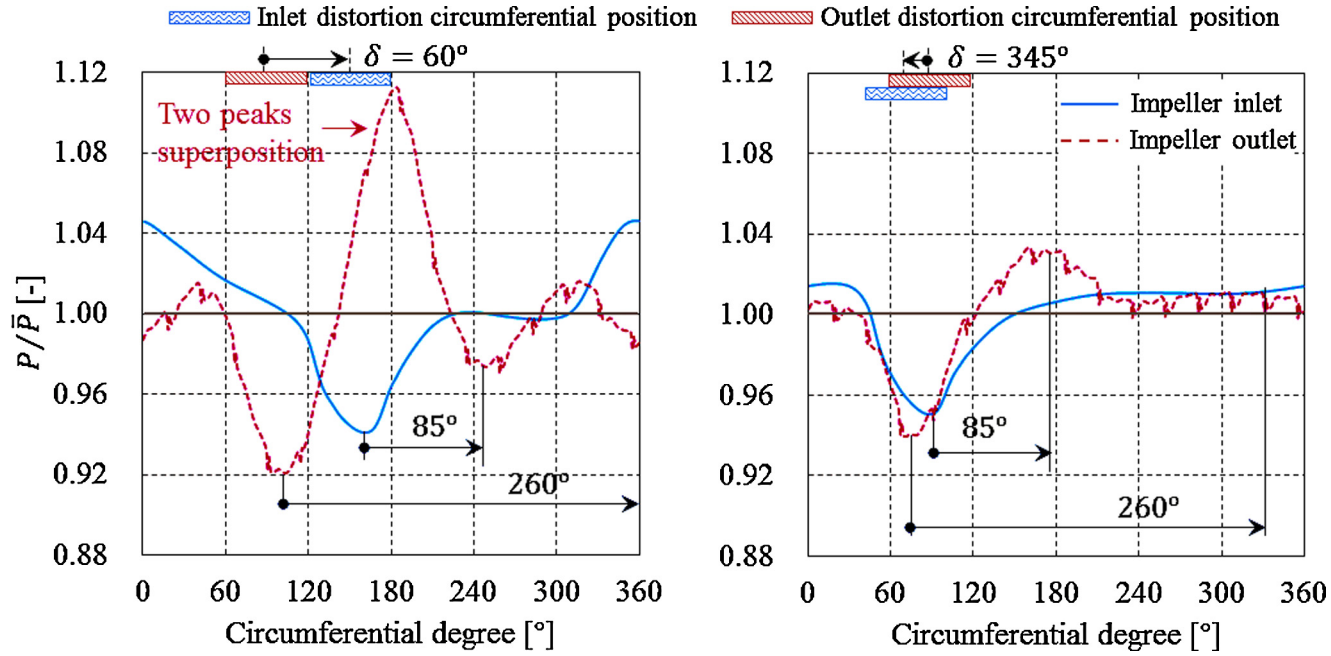

Fig. 14. Time-averaged static pressure distributions of 50% span along circumferential direction at the impeller inlet and the impeller outlet for different matching at nominal rotation speed (the impeller rotation direction is from 0 to 360°).

$$W_2 = 0.7W_1 \tag{15}$$

$$V_{m2} = W_2 \times \cos\beta_{k2} \tag{16}$$

$$\sigma = 1 - \frac{\sqrt{\cos\beta_{k2}/Z^{0.7}}}{1 - \frac{V_{m2}}{U_2}\tan\beta_{k2}} \tag{17}$$

$$U_2 = \frac{n}{60} \times 2\pi \times R_2 \tag{18}$$

$$V_{u2} = \sigma \times (U_2 - W_2 \times \sin(\beta_{k2})) \tag{19}$$

$$V_2 = \sqrt{V_{m2}^2 + V_{u2}^2} \tag{20}$$

The results of estimate formula and unsteady full-annular simulation are compared at 0.6, 0.8, 1.0 and 1.2 nominal rotation speed in Fig. 16 It demonstrates that the estimate formula is useful in predicting inlet distortion angular shift and can be used to get the best matching of inlet and outlet distortions.

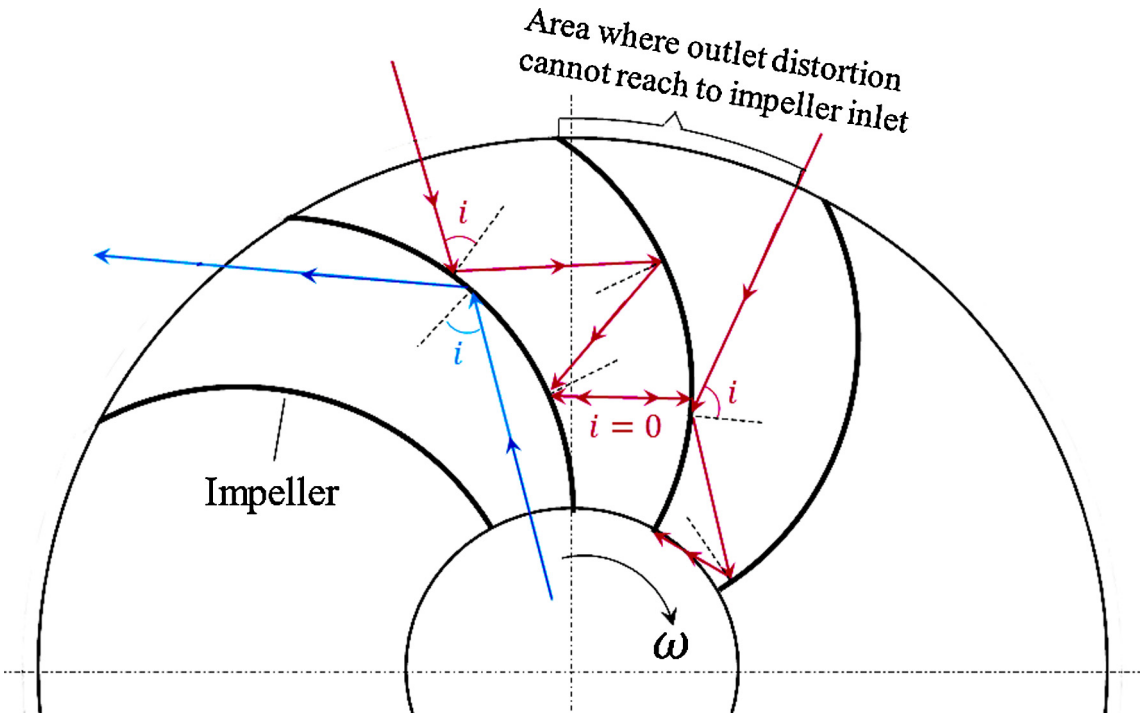

Fig. 15. Sketch map of distorted pressure wave transfer in the impeller.

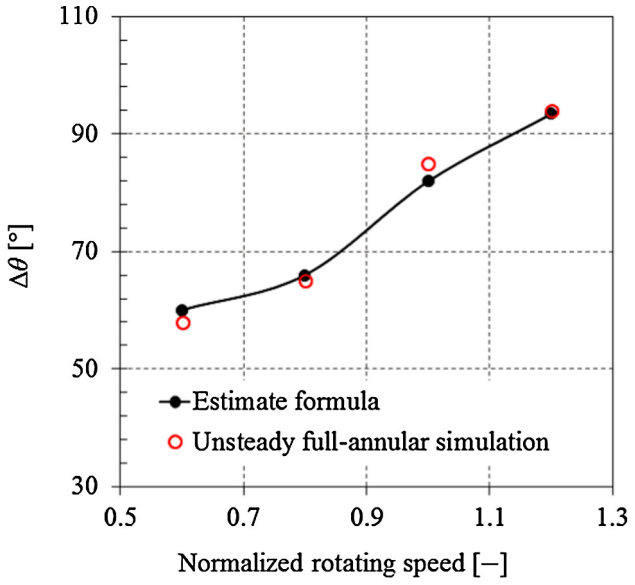

Fig. 16. Results comparison between estimate formula and unsteady full-annular simulation.

5. Conclusions

Through adding square wave distortions to the compressor inlet and outlet to simulate the distortions induced by upstream inlet bend pipes, struts and downstream volute, this paper investigates the matching of inlet and outlet distortions in centrifugal compressors using full-annular unsteady simulations in efficiency terms. Except for the compressor distorted inlet and outlet boundary condition which are determined by upstream and downstream components, the parameter distributions at impeller outlet (diffuser inlet) appear diverse for the different matching of inlet and outlet distortions. Some conclusions are drawn as follows:

(1). The matching of inlet and outlet distortions does have a large influence on the compressor performance. When the mass flow decreases, the efficiency difference becomes larger. For the cases studied in this paper, the highest efficiency difference is 0.67% at 0.8 nominal rotation speed and 1.16% at nominal rotation speed.

(2). The matching can be divided into three types. One is the best matching, where the distortions have an interaction to neutralize each other (peak and trough superpose) and limit the distortion region to a minimum at impeller outlet (diffuser outlet), so it is an expected matching. The other is the avoided matching, where the distortions have an interaction to superpose each other (peaks or troughs superpose) and lead to a large fluctuating parameter distribution at impeller outlet (diffuser inlet). The last is the mediocre matching, where the distortions have no interference and the compressor performance of this matching falls in between the best matching and the avoid matching. This can be used as the matching criteria for inlet and outlet distortions.

(3). The critical factor of how can we get the best matching is to know the angular shift of inlet distortion. But the angular shift is not fixed and it will change with impeller rotation speed. According to the sound wave theory, an estimate formula is established to provide useful guidance for the matching of inlet and outlet distortions.

Acknowledgements

This work was supported by the State Key Laboratory of Automotive Safety and Energy under Project No. KF16112. The authors would also like to thank the Institute of Jet Propulsion and Turbomachinery of RWTH Aachen, Germany, for providing the test case *RADIVER*.

References

[1] D. Vittorini, R. Cipollone, Financial analysis of energy saving via compressor replacement in industry, Energy 113 (2016) 809–820, https://doi.org/10.1016/j.energy.2016.07.073.

[2] P.J. Hotchkiss, C.J. Meyer, T.W. Von Backström, Numerical investigation into the effect of cross-flow on the performance of axial flow fans in forced draught air-cooled heat exchangers, Appl. Therm. Eng. 26 (2006) 200–208, https://doi.org/10.1016/j.applthermaleng.2005.05.012.

[3] V.J. Fidalgo, C.A. Hall, Y. Colin, A study of fan-distortion interaction within the NASA Rotor 67 transonic stage, J. Turbomach. 134 (2012) 51011, https://doi.org/10.1115/1.4003850.

[4] J.R. Brossman, P.R. Ball, N.R. Smith, J.C. Methel, N.L. Key, Sensitivity of multistage compressor performance to inlet boundary conditions, J. Propul. Power 30 (2014) 407–415, https://doi.org/10.2514/1.B34742.

[5] N. Reuβ, C. Mundt, Experimental investigations of pressure distortions on the high-pressure compressor operating behavior, J. Propul. Power 25 (2009) 653–667, https://doi.org/10.2514/1.37412.

[6] R. Bontempo, M. Cardone, M. Manna, G. Vorraro, Steady and unsteady experimental analysis of a turbocharger for automotive applications, Energy Convers. Manage. 99 (2015) 72–80, https://doi.org/10.1016/j.enconman.2015.04.025.

[7] S.M. Moosania, X. Zheng, Effect of internal heat leakage on the performance of a high pressure ratio centrifugal compressor, Appl. Therm. Eng. 111 (2017) 317–324, https://doi.org/10.1016/j.applthermaleng.2016.09.030.

[8] N.N. Bayomi, A. Abdel Hafiz, A.M. Osman, Effect of inlet straighteners on centrifugal fan performance, Energy Convers. Manage. 47 (2006) 3307–3318, https://doi.org/10.1016/j.enconman.2006.01.003.

[9] M. Enayet, M. Gibson, A. Taylor, Laser-Dopper measurements of laminar and turbulent flow in a pipe bend, Int. J. Heat Fluid Flow 3 (1982) 213–219, https://doi.org/10.1016/0142-727X(82)90024-8.

[10] K. Sudo, M. Sumida, H. Hibara, Experimental investigation on turbulent flow in a circular-sectioned 90-degree bend, Exp. Fluids 25 (1998) 42–49, https://doi.org/10.1007/s003480050206.

[11] F.U. Lou, J.C. Fabian, N.L. Key, Experimental investigation of flow distortion in an auxiliary-power-unit-style inlet system, J. Propul. Power 32 (2016) 892–902, https://doi.org/10.2514/1.B35948.

[12] J. Lu, L. Zheng, Z. Wang, L. Wang, C. Yan, Experimental investigation on interactions between a two-phase multi-tube pulse detonation combustor and a centrifugal compressor, Appl. Therm. Eng. 113 (2017) 426–434, https://doi.org/10.1016/j.applthermaleng.2016.10.188.

[13] Y. Lin, X. Zheng, L. Jin, H. Tamaki, T. Kawakubo, A novel experimental method to evaluate the impact of volute's asymmetry on the performance of a high pressure ratio turbocharger compressor, Sci. China Technol. Sci. 55 (2012) 1695–1700, https://doi.org/10.1007/s11431-012-4822-9.

[14] X. Zheng, Y. Lin, Z. Sun, Effects of volute's asymmetry on the performance of a turbocharger centrifugal compressor, Proc. Inst. Mech. Eng., Part G: J. Aerosp. Eng. (2016) 1–12, https://doi.org/10.1177/0954410016670418.

[15] A. Reunanen, H. Pitkfinen, H. Heiska, Computation and experiment comparison of different volute geometries in a radial compressor, in: ASME Turbo Expo, 2000, pp. 1–10.

[16] C. Hariharan, M. Govardhan, Improving performance of an industrial centrifugal blower with parallel wall volutes, Appl. Therm. Eng. 109 (2016) 53–64, https://doi.org/10.1016/j.applthermaleng.2016.08.045.

[17] M. Yang, R. Martinez-Botas, Y. Zhang, X. Zheng, Effect of self-recirculation-casing treatment on high pressure ratio centrifugal compressor, J. Propul. Power 32 (2016) 1–9, https://doi.org/10.2514/1.B35438.

[18] X. Zheng, Y. Zhang, M. Yang, T. Bamba, H. Tamaki, Stability improvement of high-pressure-ratio turbocharger centrifugal compressor by asymmetrical flow control-Part II: non-axisymmetrical self-recirculation casing treatment, J. Turbomach. 135 (2013) 0210061–0210069, https://doi.org/10.1115/1.4006636.

[19] C.M. Van Schalkwyk, J.D. Paduano, E.M. Greitzer, A.H. Epstein, Active stabilization of axial compressors with circumferential inlet distortion, J. Turbomach. 120 (1998) 431–439, https://doi.org/10.1115/97-GT-279.

[20] M. Yang, X. Zheng, Y. Zhang, T. Bamba, H. Tamaki, J. Huenteler, Z. Li, Stability improvement of high-pressure-ratio turbocharger centrifugal compressor by asymmetric flow control – Part I: non-axisymmetrical flow in centrifugal compressor, J. Turbomach. 135 (2013) 1–9, https://doi.org/10.1115/1.4006636.

[21] SAE International, Gas Turbine Engine Inlet Flow Distortion Guidelines, 2011.

[22] X. Zheng, L. Jin, H. Tamaki, Influence of volute-induced distortion on the performance of a high-pressure-ratio centrifugal compressor with a vaneless diffuser for turbocharger applications, Proc. Inst. Mech. Eng., Part A: J. Power Energy 228 (2014) 440–450, https://doi.org/10.1177/0957650913519984.

[23] C. Weiβ, H. Thermann, R. Niehuis, Numerical investigation of the influence of the tip clearance on wake formation inside a radial impeller, in: ASME Turbo Expo, 2003, pp. 1–11.

[24] F.J. Wiesner, A review of slip factors for centrifugal compressors, J. Eng. Power 89 (1967) 558–572, https://doi.org/10.1115/1.3616734.